In-situ Synthesis of Zirconium Oxycarbide by Electroreduction of ZrO2/C in Molten Salt

Xianwei Su
Zhengzhou University
Xiaojia Shang
Zhengzhou University
Yusi Che
Zhengzhou University
Shaolong Li
Zhengzhou University
Jianxun Song (jianxun.song@zzu.edu.cn)
Henan Province Industrial Technology Research Institute of Resources and Materials, Zhengzhou University, Science Road 100, Zhengzhou, Henan 450001, China
Jilin He
Zhengzhou University

Research Article

Keywords: In-situ synthesis, molten salt, zirconium oxycarbide, electroreduction

Posted Date: April 3rd, 2021

DOI: https://doi.org/10.21203/rs.3.rs-376923/v1

Version of Record: A version of this preprint was published at Ceramics International on April 1st, 2021.
See the published version at https://doi.org/10.1016/j.ceramint.2021.04.156.

In-situ synthesis of zirconium oxycarbide by electroreduction of ZrO_2/C in molten salt

Xianwei Su[a, b], Xiaojia Shang[a], Yusi Che[a], Shaolong Li[a], Jianxun Song[a†], and Jilin He[a, b]

[a]*Henan Province Industrial Technology Research Institute of Resources and Materials, Zhengzhou University, Science Road 100, Zhengzhou, Henan 450001, China*

[b]*School of Material Science and Engineering, Zhengzhou University, Science Road 100, Zhengzhou, Henan 450001, China*

[†]Corresponding author: jianxun.song@zzu.edu.cn (J. Song)

Abstract:

Homogenous ZrC_xO_y powders have been successfully synthesized by *in-situ* electro-reduction of solid ZrO_2-C composite precursors in molten $CaCl_2$. The effect of applied cell voltage and molar ratio of ZrO_2 to C on preparation of ZrC_xO_y were investigated. The reduction pathway of the composite electrode was studied based on the analysis of intermediate products using X-ray diffraction (XRD) and scanning electron microscopy (SEM). The results show that ZrO_2 is firstly converted to $CaZrO_3$. The resulting $CaZrO_3$ is then reduced to ZrC_xO_y. The ZrC_xO_y formation is dramatically influenced by electrolysis voltage and molar ratio of ZrO_2 to C: a higher cell voltage and lower molar ratio of the ZrO_2 to C are more preferable for the formation of ZrC_xO_y powder. Homogenous ZrC_xO_y powders with particle size of ~100 nm are synthesized by ZrO_2 /C starting elemental powders in $CaCl_2$ molten salt at 1123 K for more than 3 h, when the cell voltage is 3.0 V and the molar ratio of the ZrO_2 to carbon starting materials is 1:1.0.

Keywords: *In-situ* synthesis, molten salt, zirconium oxycarbide, electroreduction

1 Introduction

Metal carbides like TiC, Mo_2C or ZrC exhibit excellent thermomechanical properties at high temperature such as elastic properties, creep and corrosion resistance [1]. Therefore, these refractory materials can be used as structural materials for furnace units or as plasma arc electrodes. In addition, ZrC-based materials are also candidates for future nuclear reactor fuel shielding materials [2]. However, there will always be some oxygen impurities (such as ZrO_2) on the surface of ZrC particles, and oxygen atoms can replace carbon atoms in the ZrC lattice to form an oxycarbide solid solution (ZrC_xO_y) [3, 4]. Researchers already have a certain

understanding of several of the mixed transition metal-based carbon-oxygen compounds, including "TiC_xO_y" and "MoC_xO_y", x and y, which represent variable compositions. These zirconium oxycarbide are composed of ZrC and ZrO_2 and have the properties of these two materials - carbides generally have better conductivity [5, 6], while ZrO_2 has higher ceramic stability and is also a commonly used catalyst and carrier material in catalysis. In our recent work, the ZrC_xO_y was applied as consumable anode for zirconium extraction [7].

The traditional method of synthesizing zirconium oxycarbide is a solid-state synthesis method, which requires high temperature (~2000 K) and high pressure to achieve the necessary high solid state diffusion rates [8]. However, due to the high temperature, the specific parts of the prepared powder will inevitably degrade [9]. During the carbothermal reaction, the amount of carbon is the key to control the synthesis composition. The reaction mechanism has been deeply studied and discussed [8, 10, 11].

Gendre et al. [12] and Barnier et al. [13] used spark plasma sintering (SPS) to prepare ZrC_xO_y powders. The resulting powders have a better microstructure than hot pressing, but it still consumes a lot of energy during synthesis. The other commonly used method to synthesize different ceramics (including carbon compounds) is the gelation procedure, which is simple and has been used for a long time [14]. This synthesis method of zirconium carbide and oxycarbide relies on the use of organic solvents and reactants, which are more complex and environmentally unfriendly than water-based synthesis [15]. However, it is difficult to form zirconium dioxide species in an aqueous solution [16]. Therefore, it is necessary to develop new technologies and methods to reduce energy consumption and environmental pollution during the preparation of zirconium carbide and oxycarbide.

In recent years, researchers have studied and proposed a series of molten salt electrolysis processes to prepare carbide materials [17-20]. Molten salt electrolysis provides a convenient and fairly easy way to obtain carbide materials. It was reported that MC_xO_y and MC_x have been synthesized by electrolysis using the mixture of MO_2 and C as precursor in molten chloride [19, 21-26]. Electrolytic synthesis of MC_xO_y is a process of removing O^{2-} from MO_x and carbon complexes. Therefore, the composition of the electrolytic product depends on the electrolysis time and the cathode overpotential, and is also related to the ratio of the ingredients in the raw materials. However, the mechanism of electrolytic synthesis of ZrC_xO_y have not been

systematically discussed. For instance, the transformation form of Zr element and the role of C during the synthesis process. Thus, it is necessary to conduct a detailed study on the synthesis mechanism of ZrC_xO_y.

In the present work, ZrC_xO_y composites have been tried to be prepared by directly electrolyzing ZrO_2 and graphite precursors in $CaCl_2$ molten salts. The constant cell voltage of electrolysis and the ratio of ZrO_2 and carbon in the precursor were changed to study their influence on the ZrC_xO_y synthesis process.

2 Experimental

2.1 Cathode preparation

ZrO_2 (purity >99.9%) and C (purity >99%) powders were purchased from Aladdin Biochemical Technology, Shanghai, China. ZrO_2 and C powders with the different ratio of 1:0.5, 1:0.8, 1:1.0 and 1:2.0 was mixed by ball milling for 6 h at 180 r/min, and alcohol was added to the nylon bottle as dispersant. After being collected from the bottle and dried in the air at 333 K, the mixture powder was molded into granules with a diameter of 12.5 mm and a height of 5 mm under a pressure of about 200 MPa by a manual tablet press. Before the electrochemical synthesis of ZrC_xO_y, holes were punched at the edges of the pellets to fix the current collector as a cathode with a nickel-chromium alloy wire, and a high-purity C rod (φ5 mm) was used as the anode.

2.2 Electrolysis process

The electrolysis experiment was carried out in a vertical tubular resistance furnace. $CaCl_2$ (120 g, supplied by Shanghai Macklin Biochemical Co., Ltd. analytical grade ≥99.5%) molten salt was used as reaction medium, which was placed in a corundum crucible (the inner diameter of the crucible was 75 mm and the height was 95 mm). And then, the corundum crucible was placed in the resistance furnace. The reactor was then heated to 1123 K at a ramp of 6 K/min in a flowing argon atmosphere. In order to remove the remaining water from the $CaCl_2$ molten salt, the salt was pre-melted at 1123 K for 4.0 hours.

Voltage-dependent and ratio-dependent electrolysis of ZrO_2 and C composite pellets were carried out at the same time. After electrolysis, the electrode was pulled out of the molten salt, and then taken out of the reactor after the sample cooled to room temperature in an argon

atmosphere. The cooled products were washed by distilled water to remove the $CaCl_2$ thoroughly and then dried in an oven at 333 K. Finally, the sample was ground into fine powder.

2.3 Materials characterization

The phase composition of cooled electrolytic products was characterized by X-ray Diffraction (XRD-6100, SHIMADZU). The Scanning Electron Microscopy (SEM, FEI Quanta 250FEG) coupled with Energy Dispersive Spectrometer (EDS) was carried out to observe the microstructure and element distribution.

3 Results and discussion

3.1 Voltage-dependent constant-voltage electrolysis

According to the Gibbs free energy data at 1123 K from HSC Chemistry 7.0, the decomposition voltages of $CaCl_2$ and ZrO_2 were calculated to be 3.2 V and 2.3 V, respectively. Therefore, the electrolysis voltages were controlled in the range between 2.6 V and 3.0 V. In the voltage-dependent electrolysis, the electrolysis duration and temperature remained the same, i.e. 10 h and 1123 K, respectively.

Fig. 1 presents the XRD patterns of corresponding samples. ZrC_xO_y can be obtained over the voltage range from 2.6 V to 3.0 V. When the electrolysis voltage is 2.8 V and 3.0 V, the electrolysis products are all ZrC_xO_y. However, a large amount of $CaZrO_3$ is present in the samples prepared at 2.6 V. This phenomenon indicates that the phase composition of electrolytic products is highly dependent on electrolysis voltage.

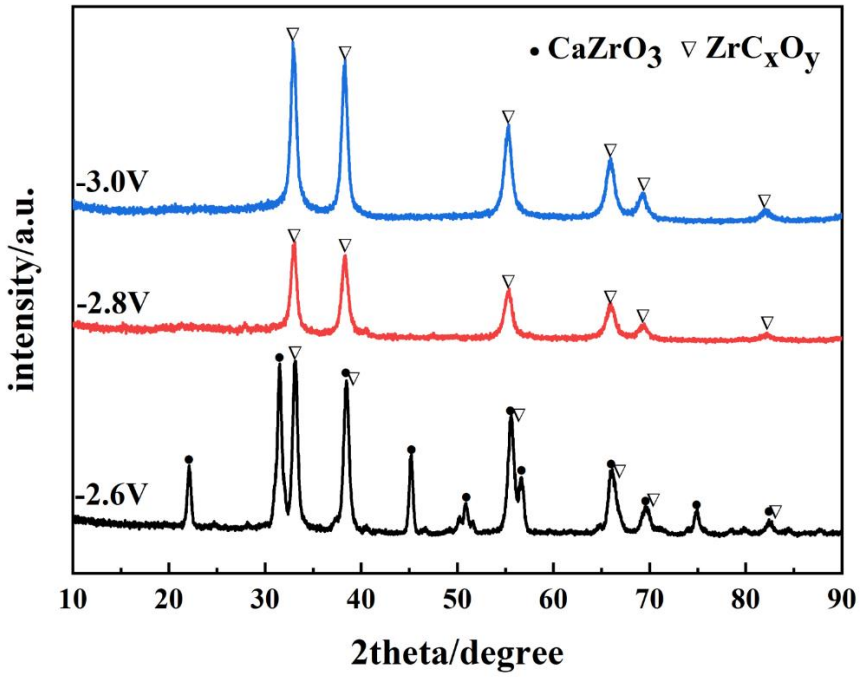

Fig. 1. The XRD patterns of ZrC_xO_y synthesized by electrolysis at different voltages (-2.6 V, -2.8 V, -3.0 V) with ZrO_2-C as the cathode and C rod as the anode for 10 hours.

In order to clarify the formation mechanism of $CaZrO_3$, the chemical stability of ZrO_2 in molten $CaCl_2$ and $CaCl_2$-CaO was studied. Fig. 2 shows the SEM images and XRD patterns of samples immersed in molten $CaCl_2$ at 1123 K for different times. As shown in Fig. 2a-f, the size of the sintered particles hardly changes, leaving pores on the surface after molten salt erosion. From the XRD patterns, the phase composition of the sample is pure ZrO_2 without phase change. The result shows that ZrO_2 has better chemical stability in molten $CaCl_2$. The corresponding SEM images and XRD patterns of samples immersed in molten $CaCl_2$-CaO at 1123 K for various times are shown in Fig. 3. There is obvious boundary between the surface layer and the inner layer, which separates the $CaZrO_3$ formed in the surface layer from the inner ZrO_2. The thickness of the $CaZrO_3$ layer increases with the immersion time. $CaZrO_3$ may be formed by the chemical reaction between ZrO_2 and CaO via Eq. (1). This reaction is thermodynamically feasible from the Gibbs free energy data at 1123 K.

$$ZrO_2 + CaO = CaZrO_3 \qquad \Delta G_{1123\ K} = -35.17\ kJ/mol \qquad (1)$$

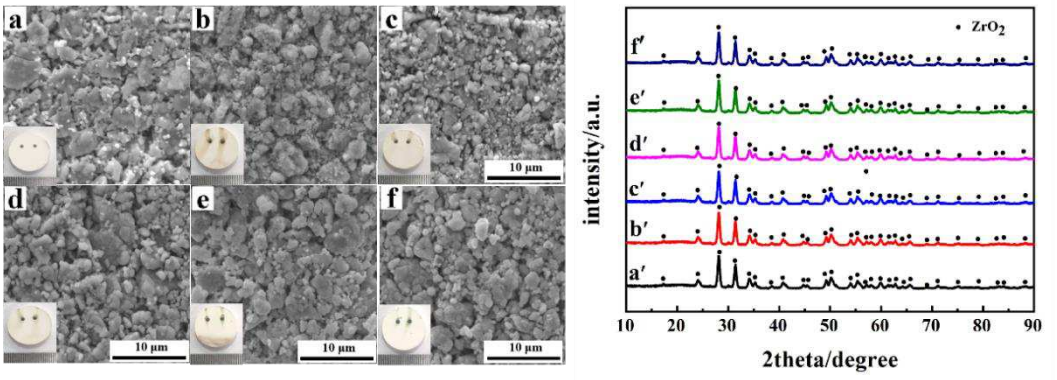

Fig. 2. SEM images and XRD patterns of ZrO_2 immersed in molten $CaCl_2$ at 1123 K for various times: (a &. a') 0 h, (b &. b') 0.5 h, (c &. c') 1 h, (d &. d') 2 h, (e &. e') 4 h, and (f &. f') 8 h.

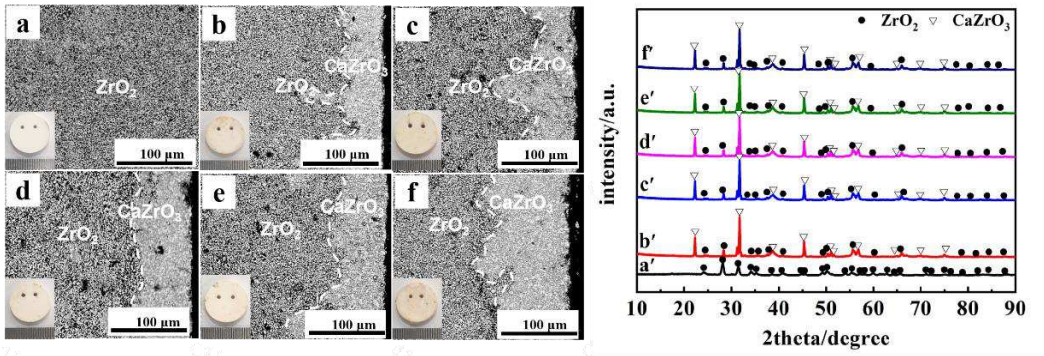

Fig. 3. The microscopic morphology and XRD patterns of ZrO_2 soaked in molten $CaCl_2$-CaO at 1123 K for various times: (a &. a') 0 h, (b &. b') 0.5 h, (c &. c') 1 h, (d &. d') 2 h, (e &. e') 4 h, and (f &. f') 8 h.

The mass change and cross-sectional micro-morphology of samples immersed in molten $CaCl_2$ and $CaCl_2$-CaO for different times are presented in Fig. 4. As illustrated in Fig. 4a-b, the mass loss of ZrO_2 immersed in molten $CaCl_2$ for 0-8 h is almost negligible, while the mass of ZrO_2 in molten $CaCl_2$-CaO increases with the increase of immersion time. From the Fig. 4c, there is a clear boundary line between $CaZrO_3$ and ZrO_2. The result further proves the above conclusion.

The electrolyte of this electrosynthesis experiment was pure $CaCl_2$, however, $CaZrO_3$ was detected although it does not contain CaO. Thus, one explanation is that the ZrO_2 as the cathode will lose some oxygen ions during electrolysis. Then, these oxygen ions combine with calcium ions in the molten salt to form CaO, which then reacts with ZrO_2 to obtain $CaZrO_3$.

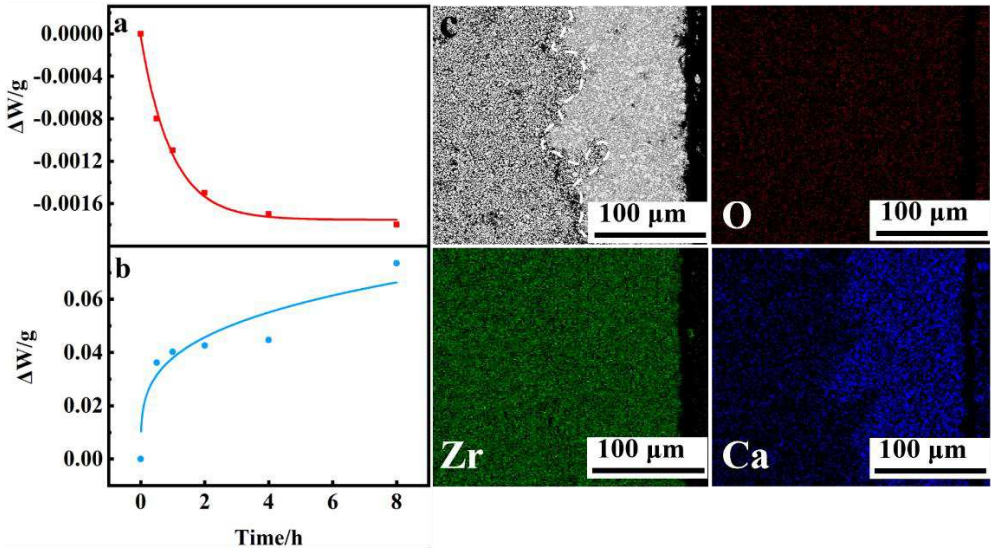

142

143 **Fig. 4.** The mass change graph of ZrO_2 immersed in different molten salts for 0~8 h at 1123

144 K: (a) $CaCl_2$ and (b) $CaCl_2$-CaO and elemental mapping of carbon, oxygen, zirconium and

145 calcium, respectively.

146 **3.2** Ratio-dependent constant-voltage electrolysis

147 To obtain the detailed information of the electro-reduction process of ZrO_2 and C composite

148 pellets in molten $CaCl_2$ at 1123 K, the pellets with different molar ratio of the ZrO_2 to C were

149 electrolyzed with a cell voltage of 3.0 V for 10 h. The XRD patterns and SEM images of

150 obtained samples are exhibited in Fig. 5.

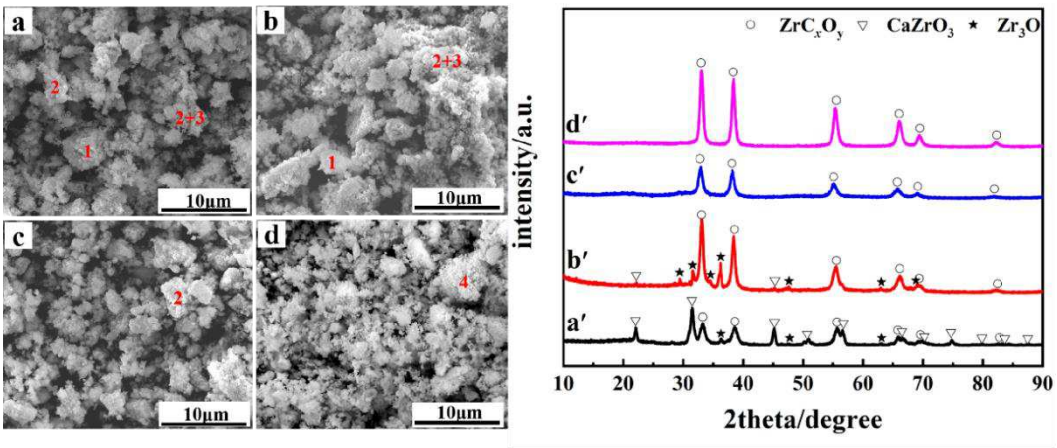

151

152 **Fig. 5.** XRD patterns and SEM images of ZrC_xO_y synthesized by electrolysis for 10 hours

153 with different molar ratio of ZrO_2 to C: (a &. a') 1:0.5, (b &. b') 1:0.8, (c &. c') 1:1.0 and (d &.

154 d') 1:2.0. (1: $CaZrO_3$; 2: ZrC_xO_y; 3: Zr_3O).

155 When the molar ratios of ZrO_2 to C are 1:0.5 and 1:0.8, Zr_3O and $CaZrO_3$ are generated in

156 addition to ZrC_xO_y. However, as the content of carbon increases to 1:1.0, the peaks related to

$CaZrO_3$ and Zr_3O disappeared and ZrC_xO_y was the only phase in the product. Fig. 5a-d shows the SEM images of samples obtained by electrolysis with different carbon content for 10 hours. It was clearly seen that there were flaky intermediate products-$CaZrO_3$, when the C was insufficient. With the increasing of C, the particles became fine and uniform, and all the cathode products were converted into ZrC_xO_y. This is consistent with the XRD results shown in Fig. 5. The existence of C promotes or participates in the formation of ZrC_xO_y. The specific process and the synthesis mechanism of ZrC_xO_y need to be obtained by studying the intermediate products in the electrolysis process.

In order to clarify the effect of C on the synthesis of ZrC_xO_y, the pellets with two different molar ratios of the ZrO_2 to C were electrolyzed with a cell voltage of 3.0 V for 0 to 10 h. Fig. 6 shows XRD patterns of samples synthesized at the molar ratio of the ZrO_2 to C of 1:0.5 and 1:1.0 at 1123 K for 0 to 10 h. As shown in Fig. 6a, the peaks of the ZrO_2 diminished with the occurrence of peaks assigned to $CaZrO_3$ and ZrC_xO_y within the first hour of electrolysis. These results suggest that $CaZrO_3$ and ZrC_xO_y were formed at the expense of ZrO_2 and C. With prolonging the electrolysis to 5 h, the peaks related to ZrO_2 disappeared while the peaks related to Zr_3O appear. After 5 h electrolysis, the peaks of ZrO_2 disappeared. The products include $CaZrO_3$, ZrC_xO_y and Zr_3O according to the XRD patterns of the products obtained after electrolysis for 5 h to 10 h. Fig. 6b shows the XRD patterns of samples synthesized at the molar ratio of the ZrO_2 to carbon of 1:1.0. Within half an hour of the electrolysis, the peaks of the ZrO_2 diminished with occurrence of $CaZrO_3$, $Ca_{0.15}Zr_{0.85}O_{1.85}$ and ZrC_xO_y. After 4 h electrolysis, ZrC_xO_y was the only phase.

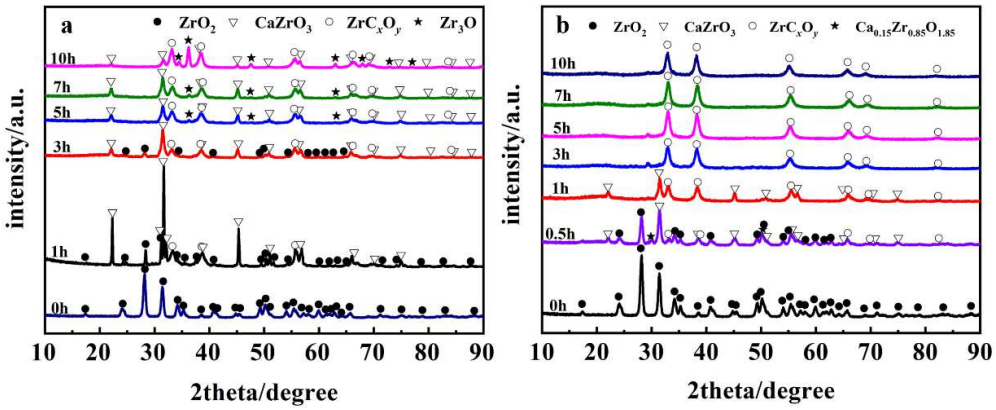

Fig. 6. XRD patterns of samples synthesized at different molar ratio of the ZrO_2 to C at 1123 K for 0 to 10 h: (a) 1:0.5 and (b) 1:1.0.

The above results provide direct insights on the formation mechanism of ZrC_xO_y from the ZrO_2 and C composite. It has been well documented that the electro-reduction process of pure ZrO_2 goes through three steps when the content of C is sufficient: $ZrO_2 \rightarrow CaZrO_3$, $Ca_{0.15}Zr_{0.85}O_{1.85}$ and ZrO_x ($1<x<2$) $\rightarrow CaZrO_3$ and $ZrC_xO_y \rightarrow ZrC_xO_y$. While the content of C is insufficient, it goes through two steps: $ZrO_2 \rightarrow CaZrO_3$ and ZrO_x ($1<x<2$) $\rightarrow CaZrO_3$, Zr_3O and ZrC_xO_y. ZrO_x was not detected in XRD because it quickly reacted with C to form ZrC_xO_y after it was produced. Zirconium dioxide in the composite is firstly transformed into various calcium intermediate phases and then the resulting calcium intermediate phases are transformed to ZrC_xO_y phase in the following electrolysis. Based on the results of ratio-dependent constant-voltage electrolysis, the reaction sequence at the cathode can be represented by reactions (2)-(9).

$$ZrO_2 = ZrO_x + (2-x)\ O^{2-} \quad (2)$$

$$O^{2-} + Ca^{2+} = CaO \qquad \Delta G_{1123K} = -517.4\ kJ/mol \quad (3)$$

$$ZrO_x + xC = ZrC_xO_y \quad (4)$$

$$ZrO_2 + CaO = CaZrO_3 \qquad \Delta G_{1123K} = -35.17\ kJ/mol \quad (5)$$

$$0.85ZrO_2 + 0.15CaO = Ca_{0.15}Zr_{0.85}O_{1.85} \quad (6)$$

$$Ca_{0.15}Zr_{0.85}O_{1.85} + 0.7CaO = 0.85CaZrO_3 \quad (7)$$

$$CaZrO_3 + xC = ZrC_xO_y + Ca^{2+} + (3-y)\ O^{2-} \quad (8)$$

$$3CaZrO_3 = Zr_3O + 3Ca^{2+} + 8O^{2-} \quad (9)$$

Fig. 7 shows the current *vs.* time plot of different molar ratios of the ZrO_2 to C. As revealed in Fig. 7a, while the molar ratio of the ZrO_2 to C is 1:0.5, the initial current is up to 1 A, and then quickly dropped to 0.4 A within 0.5 h of electrolysis. Subsequently, the current was further reduced to 0.2 A with a rather slow speed from 1 to 4 h. At last, the current retains at the value of 0.2 A. The current fluctuations in the initial period of time are related to the formation of $CaZrO_3$. With the formation of intermediates on the surface of the pellet, the transfer of oxygen ions becomes difficult and the reaction resistance increases, which resulting in a rapid drop in current. Finally, due to insufficient C content, only part of $CaZrO_3$ was converted to ZrC_xO_y. It can be clearly seen that there will be flaky intermediate product $CaZrO_3$. With prolonging the electrolysis time, the cathode products become homogeneous, and the porosity increased. Fig. 7b shows the current *vs.* time plot recorded during the electrodeoxidation process when the

molar ratio of the ZrO_2 to C is 1:1.0. The current trend is similar to that when the carbon content is insufficient, and it also goes through three stages. However, with the C content increased, $Ca_{0.15}Zr_{0.85}O_{1.85}$ was found in the intermediate product. At last, all cathode products are transformed into homogeneous nanoparticle aggregates ZrC_xO_y with uniform distribution, and with the extension of electrolysis time, the particles tend to be dispersed.

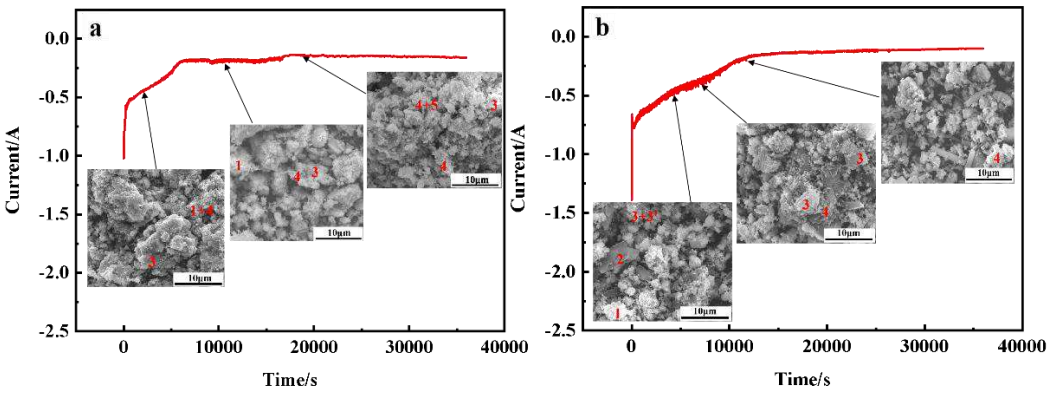

Fig. 7. Correspondence between products and I-t curve of electrolyzing ZrO_2-C: (a) 1:0.5 and (b) 1:1.0. (1: ZrO_2; 2: C; 3: $CaZrO_3$; 4: ZrC_xO_y; 5: Zr_3O).

Based on the finding and the results of XRD test in section 3.2, the electro-deoxidation process can be divided into two main stages:

Stage I: During the first hour of reduction, the $CaCl_2$ melt had yet not spread entirely into the inner of the pressed pellet, which made the reduction of pellet occurs fastly only on the surface or shallow layer. The current therefore dropped rapidly due to the slow progression penetrating into the core of the pellet. The same phenomenon was also found in other works. In this stage, the occurrence of Eq. (2), Eq. (3) and Eq. (5) is predominant. The small amount of ZrO_x generated after deoxygenation will quickly react with C to form ZrC_xO_y via Eq. (4).

Stage II: With the interior part of the pellet being infiltrated by $CaCl_2$ melt gradually, more and more C provides the conductive phase within the pellet, accelerating the electro-deoxidation rate of the interior part of the pellet. As shown in Fig. 6, the formation of zirconium oxycarbide occurs after 1 h. However, the rate of electro-deoxidization would be retarded due to the presence of zirconium oxycarbide since its higher molar volume tends to slow up the oxygen diffusion. Such a competitive relationship between C and zirconium oxycarbide exists until the depletion of C. In this stage, Eq. (8) is prevalent. At the end of this stage, the C was

entirely consumed and transformed into zirconium oxycarbide via Eq. (8). When the carbon content is insufficient, part of $CaZrO_3$ is decomposed into Zr_3O via Eq. (9).

Based on the above results, the process for the molten salt electro-synthesis of ZrC_xO_y composite powder from ZrO_2-C precursor can be summarized and schematically illustrated in Fig. 8. From the Fig. 8a, when the C content is insufficient, the process of synthesizing ZrC_xO_y is relatively complicated. Firstly, the cathode ZrO_2 is deoxidized, and O^{2-} enters the molten salt and combines with Ca^{2+} to form CaO. ZrO_x generated after deoxygenation will quickly react with C to form ZrC_xO_y. Then the remaining ZrO_2 reacts with CaO to form $CaZrO_3$. Finally, due to insufficient C content, only part of $CaZrO_3$ reacts with C to form ZrC_xO_y. Part of the remaining $CaZrO_3$ is decomposed into Zr_3O, and the other part cannot react with C and remains. The final products are ZrC_xO_y, Zr_3O and $CaZrO_3$.

Schematic diagram of ZrC_xO_y synthesis when C content is sufficient is shown in Fig. 8b. The deoxidation process in the first stage is the same as when C is insufficient. However, in addition to $CaZrO_3$, ZrO_2 will react with CaO to form another product- $Ca_{0.15}Zr_{0.85}O_{1.85}$. Then, $Ca_{0.15}Zr_{0.85}O_{1.85}$ further reacts with CaO to transform into $CaZrO_3$. Finally, all $CaZrO_3$ reacts with C to form ZrC_xO_y on account of the C content sufficient.

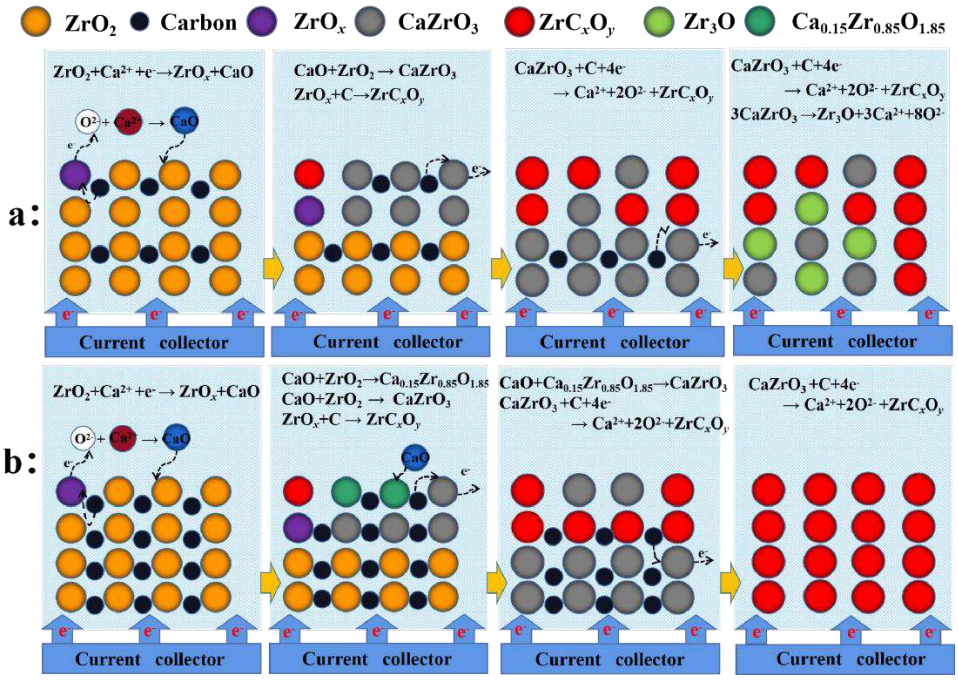

Fig. 8. Schematic diagram of electrolytic synthesis of ZrC_xO_y in molten salt using raw materials with different molar ratios of ZrO_2 and C: (a) 1:0.5; (b) 1:1.0.

4 Conclusions

Single phase ZrC_xO_y powder was synthesized *in-situ* by the electro-deoxidation of ZrO_2 and C composite at the voltage of 3.0 V in molten $CaCl_2$ salt at 1123 K when the molar ratio of the ZrO_2 to C starting materials is 1:1.0. After a carful observation, other products such as Zr_3O and $CaZrO_3$ will be formed when the ratios are 1:0.5 and 1:0.8. The mechanism of reduction ZrO_2/C was found to be split into two steps, in which the ZrO_2/C composite was firstly transformed to $CaZrO_3$, and then the $CaZrO_3$ was further reduced to ZrC_xO_y. The presence of C will promote the formation of ZrC_xO_y.

References

[1] Toth, L E. Superconducting properties of transition metal carbides and nitrides. Final report. United States: N. p., 1971.

[2] Gosset D, Dolle M, Simeone D, et al. Structural behaviour of nearly stoichiometric ZrC under ion irradiation. Nuclear Instruments & Methods in Physics Research Section B-Beam Interactions with Materials and Atoms, 2008, **266(12-13)**: 2801-2805.

[3] Antou G, Gendre M, Laborde E, et al. High temperature compressive creep of spark plasma sintered zirconium (oxy-)carbide. Materials Science and Engineering a-Structural Materials Properties Microstructure and Processing, 2014, **612**: 326-334.

[4] Sarkar S K, Miller A D, Mueller J. The solubility of oxygen in sodium. Journal of the American Ceramic Society, 1972, **55(12)**: 385-386.

[5] Modine F A, Foegelle M D, Finch C B, et al. Electrical properties of transition-metal carbides of group IV. Physical Review B Condensed Matter, 1989, **40(14)**: 9558-9564.

[6] Shul'pekov A M, Lyamina G V. Electrical and thermomechanical properties of materials based on nonstoichiometric titanium carbide prepared by self-propagating high-temperature synthesis. Inorganic Materials, 2011, **47(7)**: 722-727.

[7] Shang X, Li S, Che Y, et al. Novel extraction of Zr based on an in-situ preparation of ZrC_xO_y. Separation and Purification Technology, 10.1016/j.seppur.2020.118096.

[8] Gendre M, Maitre A, Trolliard G. Synthesis of zirconium oxycarbide (ZrC_xO_y) powders: Influence of stoichiometry on densification kinetics during spark plasma sintering and on mechanical properties. Journal of the European Ceramic Society, 2011, **31(13)**: 2377-2385.

[9] Yan Y, Huang Z, Liu X, et al. Carbothermal synthesis of ultra-fine zirconium carbide powders using inorganic precursors via sol-gel method. Journal of Sol-Gel Science and Technology, 2007, **44(1)**: 81-85.

[10] Berger L M, Gruner W, Langholf E, et al. On the mechanism of carbothermal reduction processes of TiO_2 and ZrO_2. International Journal of Refractory Metals & Hard Materials, 1999, **17(1-3)**: 235-243.

[11] Maitre A, Lefort P. Solid state reaction of zirconia with carbon. Solid State Ionics, 1997, **104(1-2)**: 109-122.

[12] Gendre M, Maitre A, Trolliard G. A study of the densification mechanisms during spark plasma sintering of zirconium (oxy-)carbide powders. Acta Materialia, 2010, **58(7)**: 2598-2609.

[13] Barnier P, Thévenot F. Synthesis and hot-pressing of single-phase ZrC_xO_y and two-phase ZrC_xO_y-ZrO_2 materials. International Journal of High Technology Ceramics, 1986, **2(4)**: 291-307.

[14] Hall, S., R., et al. The evolution of 'sol-gel' chemistry as a technique for materials synthesis. Materials Horizons, 2016.

[15] Yan C, Liu R, Cao Y, et al. Synthesis of submicrometer zirconium carbide formed from inorganic-organic hybrid precursor pyrolysis. Journal of Sol-Gel Science and Technology, 2012, **64(1)**: 251-256.

[16] Shannon R D. Revised effective ionic radii and systematic studies of interatomic distances in halides and chalcogenides. Acta Crystallographica, Section A (Crystal Physics, Diffraction, Theoretical and General Crystallography), 1976, **A32**: 751-67.

[17] Abdelkader A M. Molten salts electrochemical synthesis of Cr_2AlC. Journal of the European Ceramic Society, 2016, **36(1)**: 33-42.

[18] Abdelkader A M, Fray D J. Electrochemical synthesis of hafnium carbide powder in molten chloride bath and its densification. Journal of the European Ceramic Society, 2012, **32(16)**: 4481-4487.

[19] Liu H, Cai Y, Xu Q, et al. In situ nano-sized ZrC/ZrSi composite powder fabricated by a one-pot electrochemical process in molten salts. RSC Advances, 2017, **7(4)**: 2301-2307.

[20] Pang Z, Zou X, Zheng K, et al. Sustainable synthesis of Cr_7C_3, Cr_2AlC, and their derived porous carbons in molten salts. ACS Sustainable Chemistry & Engineering, 2018, **6(12)**: 16607-16615.

[21] Chen K, Hua Y, Xu C, et al. Preparation of TiC/SiC composites from Ti-enriched slag by an electrochemical process in molten salts. Ceramics International, 2015, **41(9)**: 11428-11435.

[22] Fan J, Yang Y, Tang D, et al. Electrochemical synthesis of nano-metallic carbides from the mixtures of metal oxide and C. Journal of the Electrochemical Society, 2017, **164(7)**: E144-E150.

[23] Tang D, Xiao W, Tian L, et al. Electrosynthesis of Ti_2CO_n from TiO_2/C composite in molten $CaCl_2$: effect of electrolysis voltage and duration. Journal of the Electrochemical Society, 2013, **160(11)**: F1192-F1196.

[24] Wang S, Wan C, Liu X, et al. Investigation on the oxidation and reduction of titanium in molten salt with the soluble TiC anode. Metallurgical and Materials Transactions E-Materials for Energy Systems, 2015, **2(4)**: 250-254.

[25] Zhang L, Wang S, Jiao S, et al. Electrochemical synthesis of titanium oxycarbide in a $CaCl_2$ based molten salt. Electrochimica Acta, 2012, **75**: 357-359.

[26] Zhou Z, Zhang Y, Dong P, et al. Electrolytic synthesis of TiC/SiC nanocomposites from high titanium slag in molten salt. Ceramics International, 2018, **44(4)**: 3596-3605.

Figures

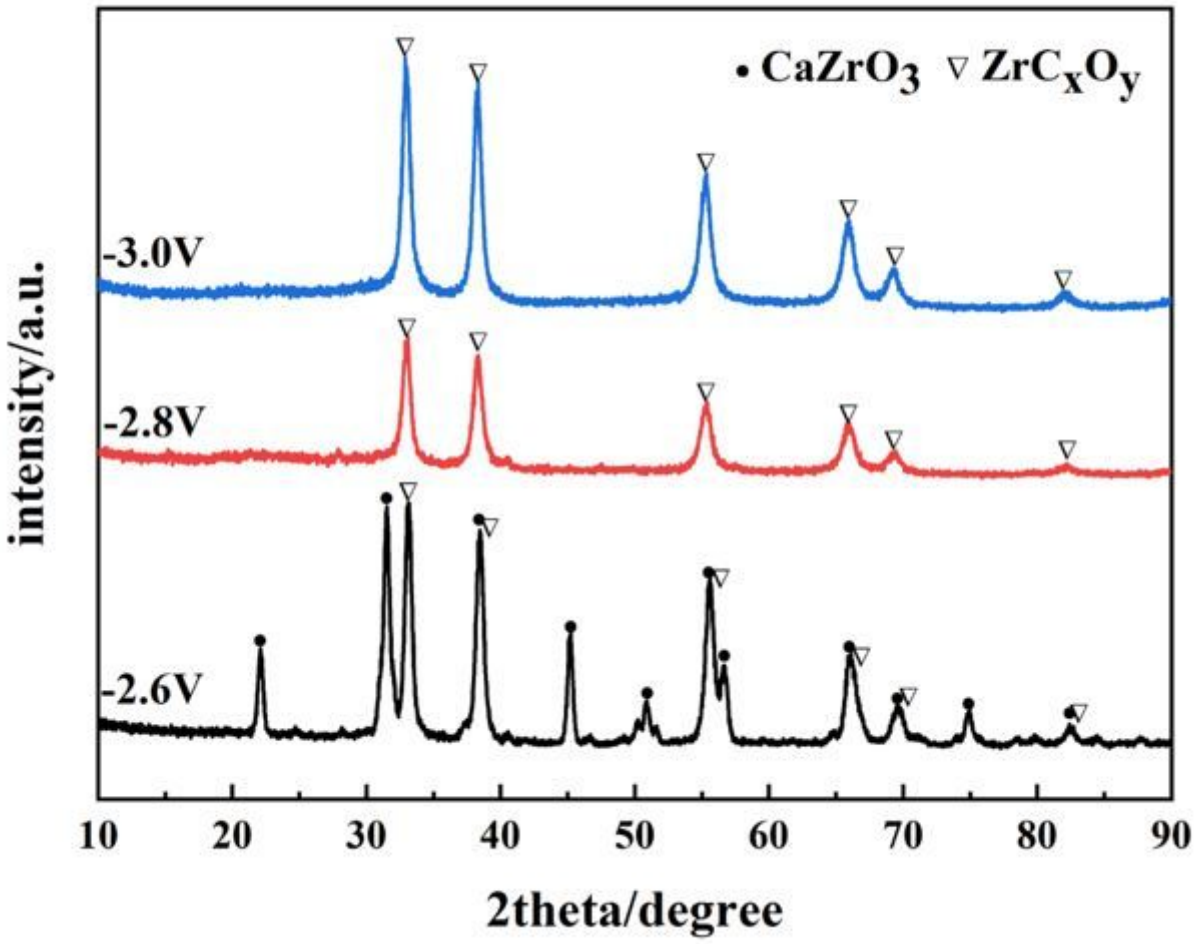

Figure 1

The XRD patterns of ZrCxOy synthesized by electrolysis at different voltages (-2.6 V, -2.8 V, -3.0 V) with ZrO2-C as the cathode and C rod as the anode for 10 hours.

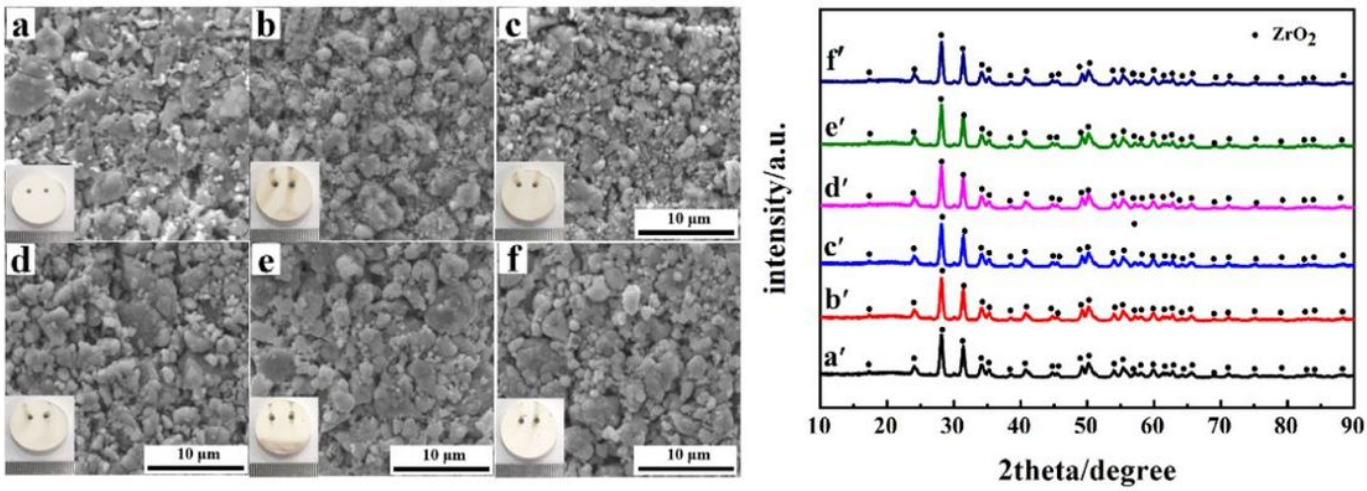

Figure 2

SEM images and XRD patterns of ZrO2 immersed in molten CaCl2 at 1123 K for various times: (a &. a') 0 h, (b &. b') 0.5 h, (c &. c') 1 h, (d &. d') 2 h, (e &. e') 4 h, and (f &. f') 8 h.

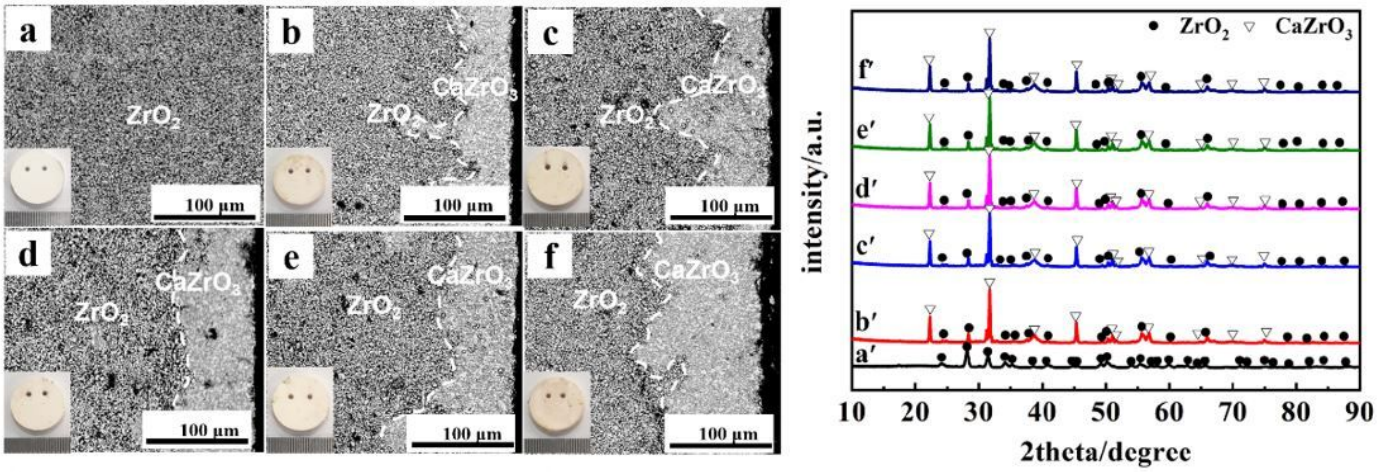

Figure 3

The microscopic morphology and XRD patterns of ZrO2 soaked in molten CaCl2-CaO at 1123 K for various times: (a &. a') 0 h, (b &. b') 0.5 h, (c &. c') 1 h, (d &. d') 2 h, (e &. e') 4 h, and (f &. f') 8 h.

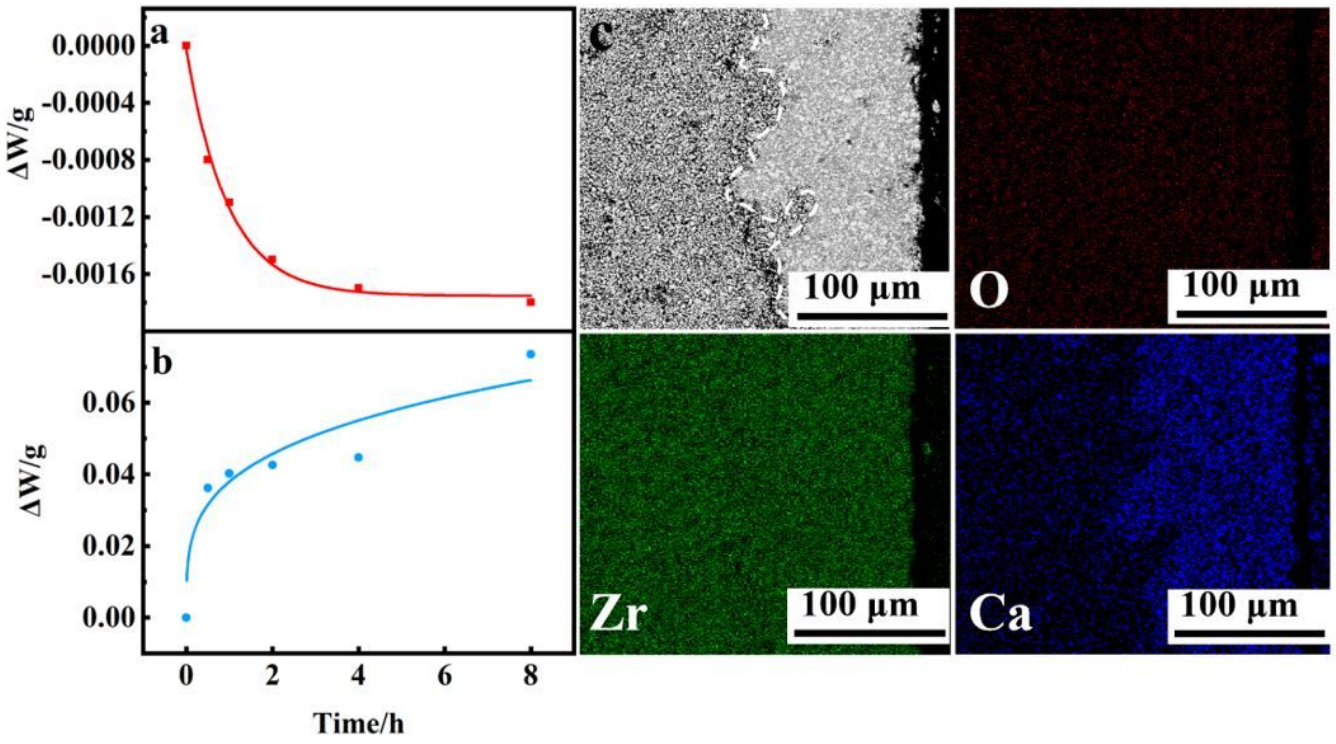

Figure 4

The mass change graph of ZrO2 immersed in different molten salts for 0~8 h at 1123 K: (a) CaCl2 and (b) CaCl2-CaO and elemental mapping of carbon, oxygen, zirconium and calcium, respectively.

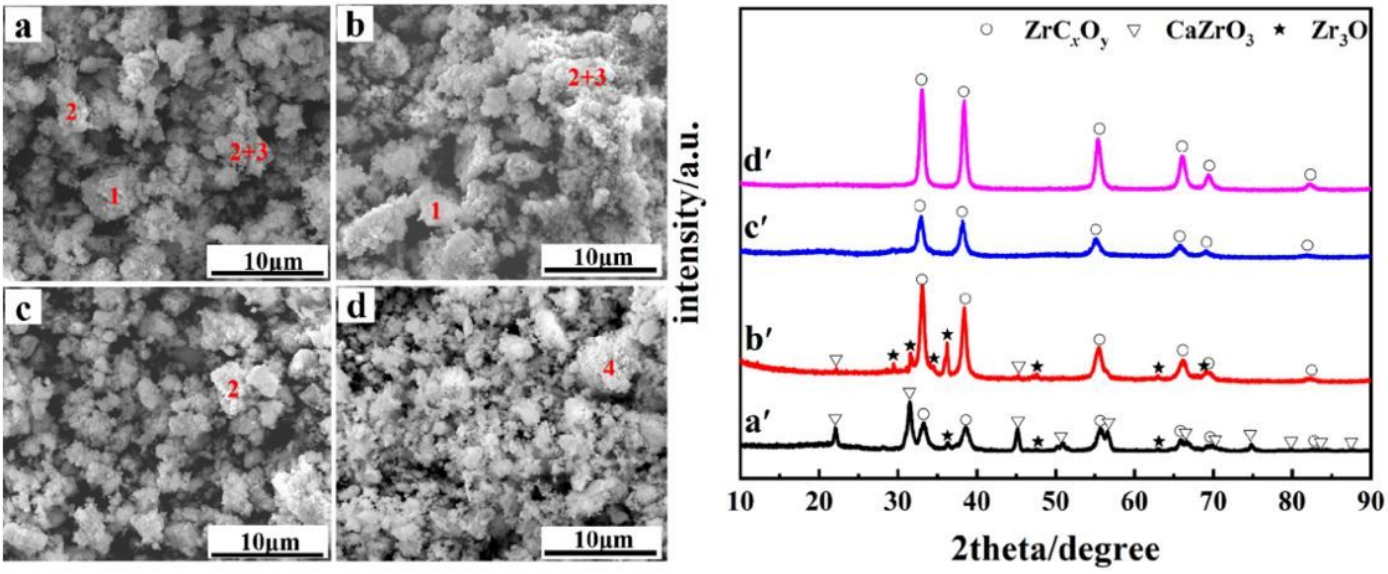

Figure 5

XRD patterns and SEM images of ZrCxOy synthesized by electrolysis for 10 hours with different molar ratio of ZrO2 to C: (a &. a') 1:0.5, (b &. b') 1:0.8, (c &. c') 1:1.0 and (d &. d') 1:2.0. (1: CaZrO3; 2: ZrCxOy; 3:

Zr3O).

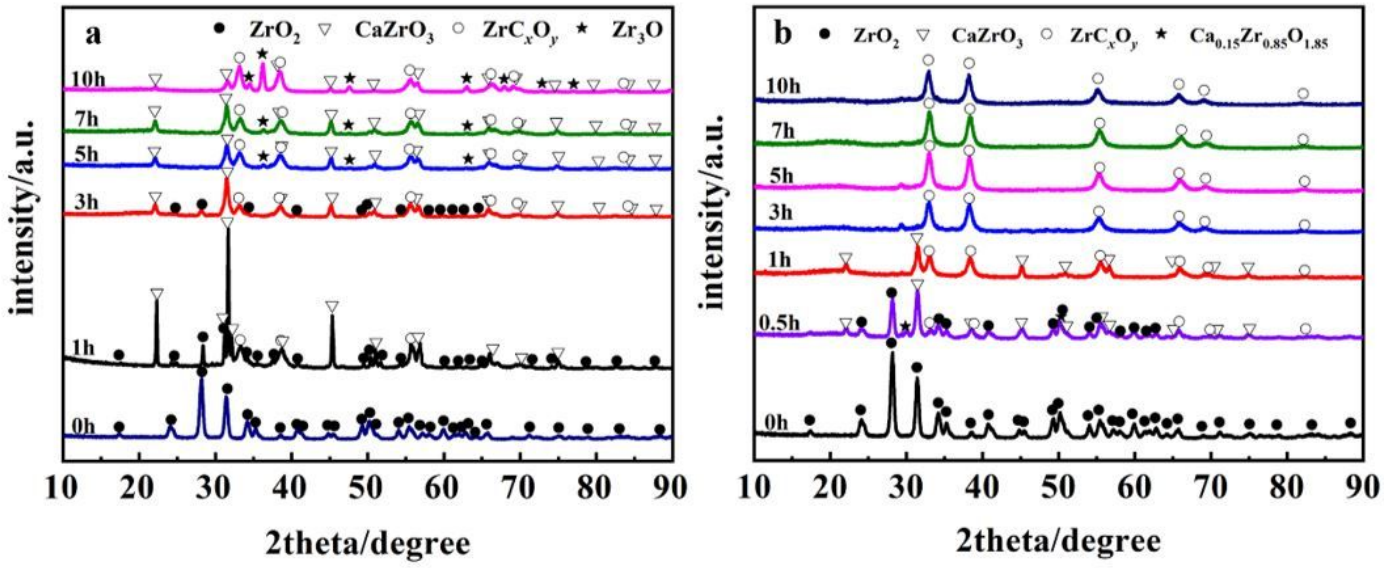

Figure 6

XRD patterns of samples synthesized at different molar ratio of the ZrO2 to C at 1123 K for 0 to 10 h: (a) 1:0.5 and (b) 1:1.0.

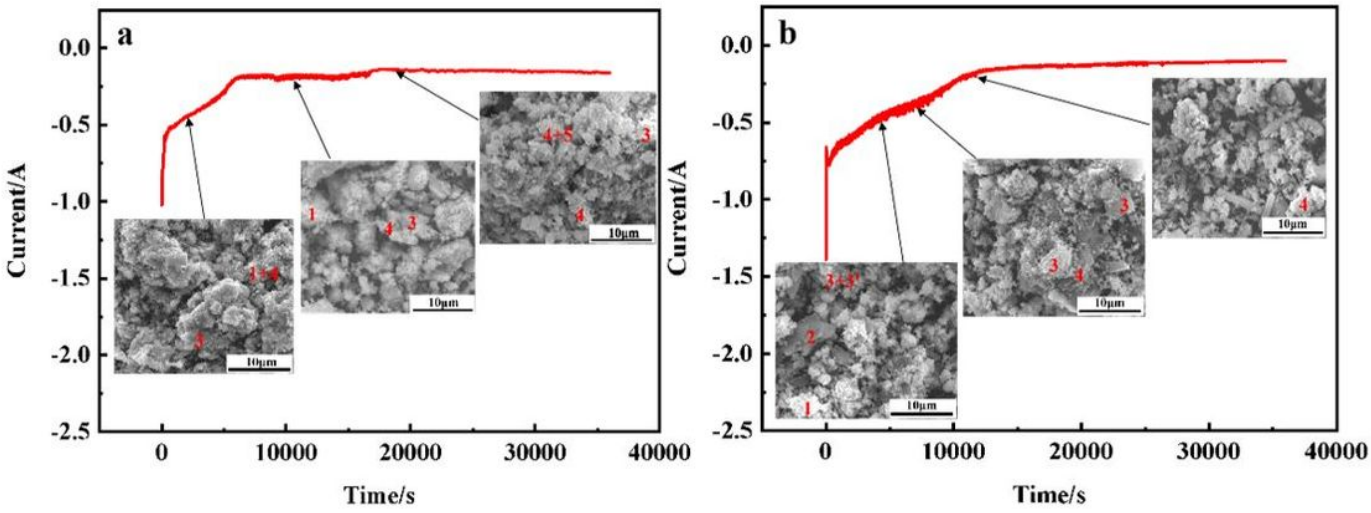

Figure 7

Correspondence between products and I-t curve of electrolyzing ZrO2-C: (a) 1:0.5 and (b) 1:1.0. (1: ZrO2; 2: C; 3: CaZrO3; 4: ZrCxOy; 5: Zr3O).

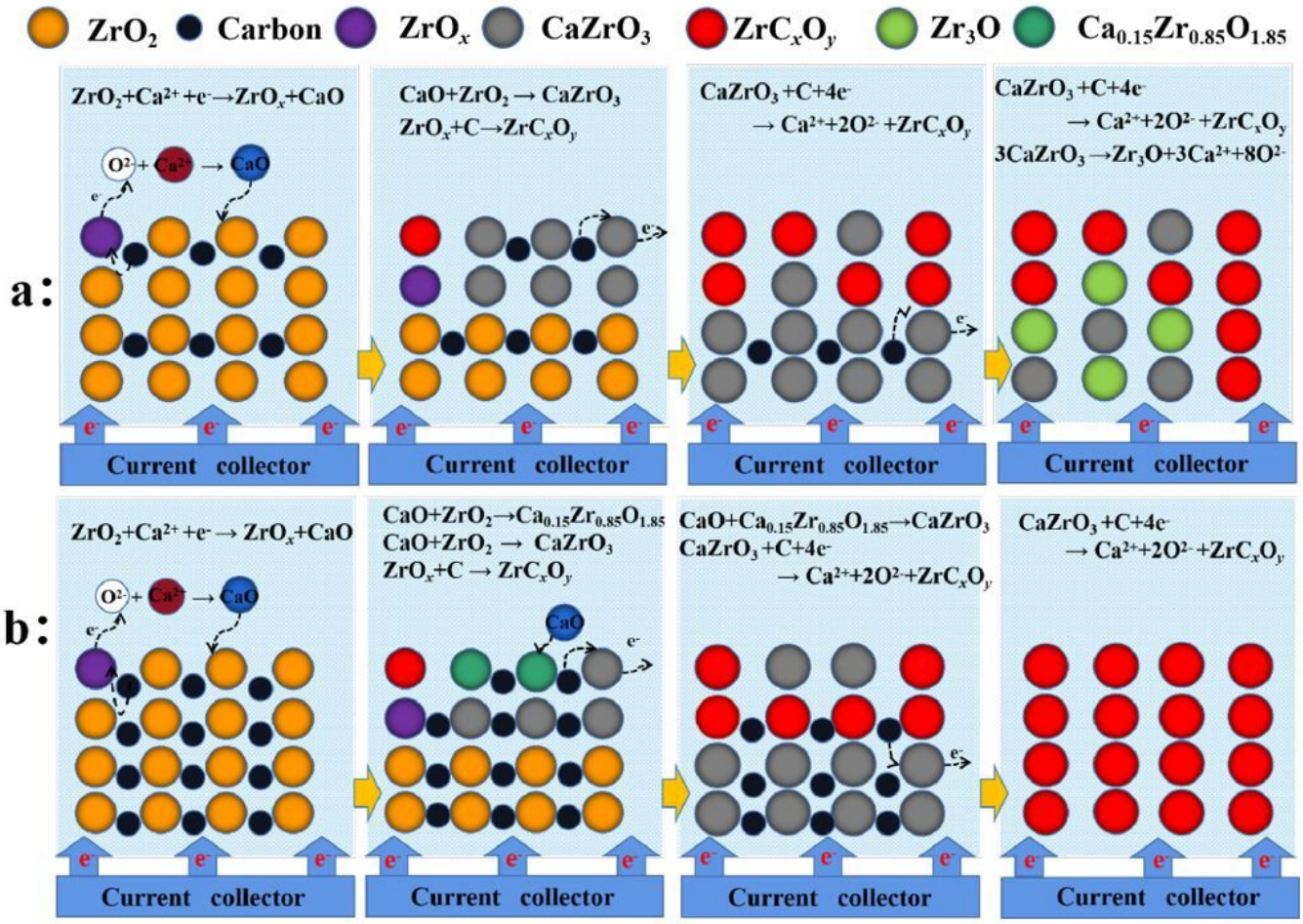

Figure 8

Schematic diagram of electrolytic synthesis of ZrCxOy in molten salt using raw materials with different molar ratios of ZrO2 and C: (a) 1:0.5; (b) 1:1.0.